Inorganic Chemistry

Communication

pubs.acs.org/IC

# Cyanide-Bridged Decanuclear Cobalt–Iron Cage

Takuya Shiga, Tamaki Tetsuka, Kanae Sakai, Yoshihiro Sekine, Masayuki Nihei, Graham N. Newton, and Hiroki Oshio*

Graduate School of Pure and Applied Sciences, University of Tsukuba, Tennodai 1-1-1, Tsukuba, Ibaraki 305-8571, Japan

Supporting Information

**ABSTRACT:** A cyanide-bridged decanuclear $[Co_6Fe_4]$ cluster was synthesized by a one-pot reaction, and the magnetic properties and electronic configuration were investigated. The complex displayed thermally controlled electron-transfer-coupled spin transition (ETCST) behavior between $Co^{III}$ low-spin–NC–$Fe^{II}$ low-spin and $Co^{II}$ high-spin–NC–$Fe^{III}$ low-spin states, as confirmed by single-crystal X-ray, magnetic, and Mössbauer analyses.

Functional molecular materials have great promise as innovative chemical compounds for the development of future electronic devices and medical products.[1] The controlled construction of highly organized molecular architectures is a necessity if species exhibiting desirable characteristics are to be reliably isolated. Synthetic techniques in supramolecular chemistry employ a variety of chemical bonds and molecular interactions, the organization of which depends on self-assembly.[2] Various molecular architectures have been constructed using ligands with strictly defined coordination modes in conjunction with the flexible coordination environments of transition-metal ions. Cagelike compounds,[3] grid complexes,[4] metal wires,[5] rotaxanes,[6] and catenanes[7] are prime examples of self-assembled species and show varied physical properties. Studies on cage compounds have focused on the templating and molecular interactions of guest molecules captured in the cavity,[8] while grid complexes have attracted a great deal of attention as molecular units for nanoscale electric devices because of the controllability of their electronic states.[9] Metal wires can exhibit interesting metal–metal bonds resulting from careful molecular design,[10] and the dynamic behavior of rotaxanes and catenanes has been studied intensely with a view to their application in molecular machines.[11]

The self-assembly of cagelike molecules has been thoroughly investigated by Fujita et al., who reported a $M_{12}L_{24}$ cage.[12] Similar transition-metal cage systems have been reported, but the vast majority were constructed from the combination of rigid, "preprogrammed" organic ligands and diamagnetic metal ions, such as $Pd^{2+}$, $Pt^{2+}$, $Cd^{2+}$, and $Zn^{2+}$.[3]

We previously reported $[Ni_6Fe_4]$ and $[Co_{10}]$ cage molecules, which were obtained by the self-assembly of chiral bidentate ligands with nickel or cobalt ions and hexacyanometalate units.[13] The $[Ni_6Fe_4]$ complexes show ferromagnetic interactions between $Ni^{II}$ and low-spin $Fe^{III}$ ions because of the orthogonality of their magnetic orbitals and constitute a rare example of magnetic cage molecules. It is important for the development of future functional cage molecules to explore the physical properties and functional behavior accessible with such species.

In this work, we extended our study of cyanide-bridged cages to synthesize a $[Co_6Fe_4]$ cage. Some cyanide-bridged cobalt–iron complexes are known to show electron-transfer-coupled spin transition (ETCST) phenomena, and such species are expected to have applications in future nanoscale switching technologies.[14] For instance, a $[Co_2Fe_2]$ square,[14a] $[Co_6Fe_8]$ macrocycles,[14b,c] and a [CoFe] one-dimensional chain[14d] have been shown to exhibit switchable magnetic properties when stimulated by temperature or light. In this paper, the synthesis, structure, and magnetic properties of a cyanide-bridged $[Co_6Fe_4]$ cage molecule are presented.

The cyanide-bridged decanuclear cage $(Et_4N)_2[\{Co(L^R)\}_6\{Fe(CN)_6\}_4](BF_4)\cdot 17CH_3OH\cdot 12H_2O$ (**1**, $[Co_6Fe_4]$) was obtained by the reaction of **2**–pyridinecarbaldehyde and *R*-(+)-phenylethylamine with $Co(BF_4)_2\cdot 6H_2O$ and $(Et_4N)_3[Fe(CN)_6]$ (Figure 1).[15] Single-crystal X-ray analysis reveals that **1** crystallized in the orthorhombic space group $P2_12_12_1$ and has a cage structure constructed from six $[Co(L^R)_2]$ and four hexacyanoferrate units, within which one tetraethylammonium cation is encapsulated. The metal arrangement is adamantane-like in topology: very close to that of the reported $[Ni_6Fe_4]$ cage molecules.[13] The cobalt ions have octahedral coordination geometries with four nitrogen donor atoms from two chiral bidentate ligands and two nitrogen donor atoms from two neighboring hexacyanoferrate units. All cobalt ions have Δ-type conformations, stabilized by π–π-stacking interactions between the phenyl moieties of the ligands in neighboring molecules. Considering the bond lengths around the cobalt centers and their distortion from perfect octahedral geometry at 100 K, three cobalt ions (Co1, Co2, and Co4) are 2+ and high-spin [HS; $d_{av\ 100\ K}(Co^{II}–L) = 2.14$ Å], while the other three (Co3, Co5, and Co6) are 3+ and low-spin [LS; $d_{av\ 100\ K}(Co^{III}–L) = 1.93$ Å]. Mössbauer data collected at 100 K suggest that all iron ions are 2+ and LS (vide infra). The combined analyses suggest that compound **1** has a $[Co^{II}(HS)_3Co^{III}(LS)_3Fe^{II}(LS)_4]$ electronic state at 100 K. Structural analysis at 291 K shows significant differences. Five cobalt ions (Co1–Co5) are divalent and HS [$d_{av\ 291\ K}(Co^{II}–L) = 2.12$ Å], while one (Co6) remains trivalent and LS [$d_{av\ 291\ K}(Co^{III}–L) = 1.90$ Å]. X-ray structural analysis is of limited utility in differentiating between $Fe^{II}$(LS) and $Fe^{III}$(LS) ions, but Mössbauer spectra at 300 K revealed their presence in a 1:1 ratio, indicating that two electron transfers lead to an electronic state of $[Co^{II}(HS)_5Co^{III}(LS)Fe^{II}(LS)_2Fe^{III}(LS)_2]$ at high temperature. The locations of the $Co^{II}$ and $Co^{III}$ ions allow us to suggest the $Fe^{II}$ and $Fe^{III}$ positions based on charge-

**Received:** April 25, 2014
**Published:** June 3, 2014





dx.doi.org/10.1021/ic500964m | *Inorg. Chem.* 2014, 53, 5899–5901

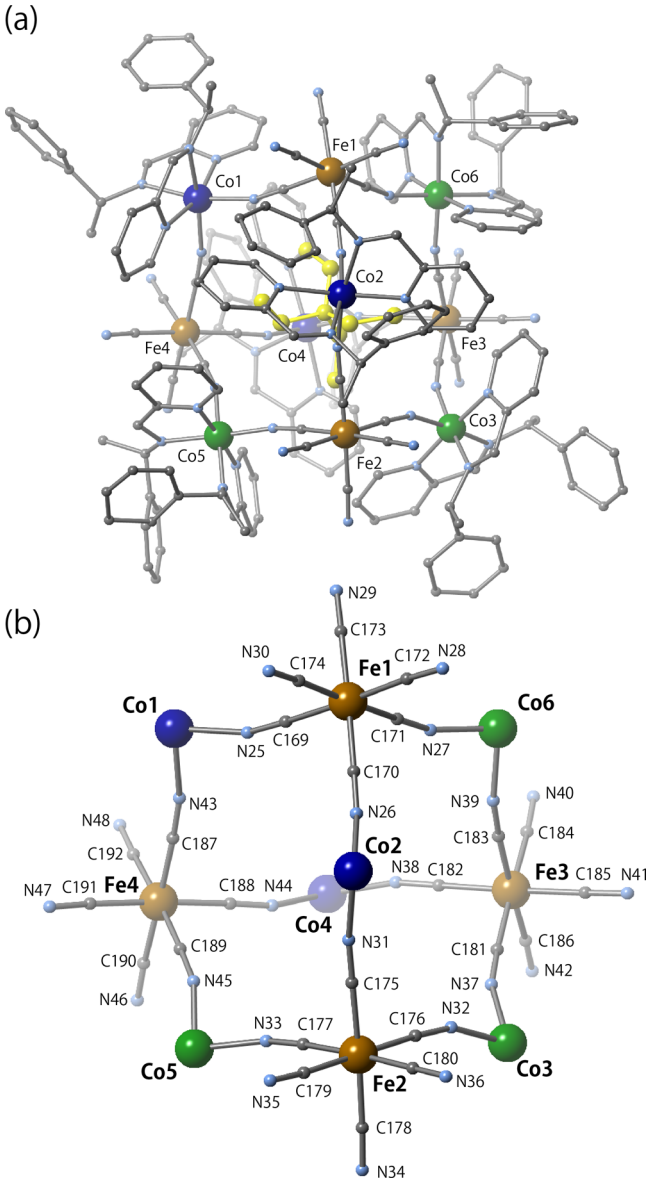


**Figure 1.** Molecular (a) and core (b) structures of **1** at 100 K. The encapsulated tetraethylammonium cation is highlighted in yellow. Hydrogen atoms, counteranions outside the cage, and solvent molecules have been omitted for clarity. Color code: C, gray; N, light blue; $Co^{II}(HS)$, blue; $Co^{III}(LS)$, green; $Fe^{II}(LS)$, brown.

repulsion considerations. Schematic representations of the metal-ion positions are provided in Figure 2 (inset).

The magnetic susceptibility of a fresh sample of **1** was measured using a sealed quartz cell, and $\chi_m T$ versus $T$ plots are shown in Figure 2. Spin transition was observed around 250 K. At 300 K, the $\chi_m T$ value of 12.42 emu mol$^{-1}$ K is close to the expected value of 12.41 emu mol$^{-1}$ K, estimated from the sum of the uncorrelated spins of five $Co^{II}(HS)$ and two $Fe^{III}(LS)$ ions ($g$ = 2.21). Lowering the temperature caused the $\chi_m T$ value to decrease, initially gradually and then more abruptly at around 250 K, before reaching a plateau below 180 K with an almost constant $\chi_m T$ value of 6.83 emu mol$^{-1}$ K, consistent with the value expected from three magnetically isolated $Co^{II}(HS)$ ions (6.83 emu mol$^{-1}$ K; $g$ = 2.20). Below 100 K, the $\chi_m T$ values decreased because of the orbital contribution of the $Co^{II}$ ions. The cooling and heating processes for the fresh sample were

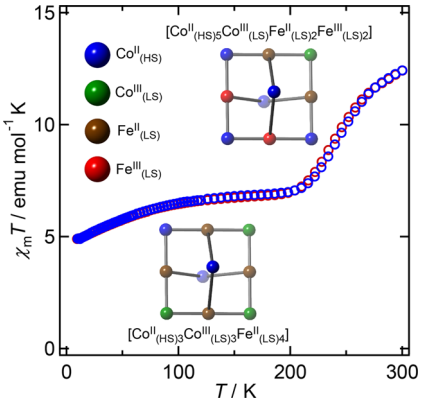


**Figure 2.** Plots of $\chi_m T$ versus $T$ for **1** (fresh sample). Red and blue markers indicate the heating and cooling processes, respectively. Inset: schematic diagrams showing the spin-state changes associated with the ETCST.

reversible to 300 K and confirm the ETCST suggested by the structural data.

While over the relatively short time scale of magnetic susceptibility measurements the phase transition was reversible, desolvation effects were apparent in the Mössbauer analyses. Measurements on a fresh sample of **1** conducted at 100 K revealed one doublet corresponding to $Fe^{II}(LS)$ ($\delta_{IS}$ = 0.0 mm s$^{-1}$; $\Delta E_Q$ = 0.16 mm s$^{-1}$) consistent with the $[Co^{II}(HS)_3Co^{III}(LS)_3Fe^{II}(LS)_4]$ assignment indicated by the susceptibility data (Figure 3). However, measurement at 300 K for 1 week caused an irreversible transition to the high-temperature phase. Solvent molecules in the crystal lattice can be removed by sample drying, and the formula of the dried

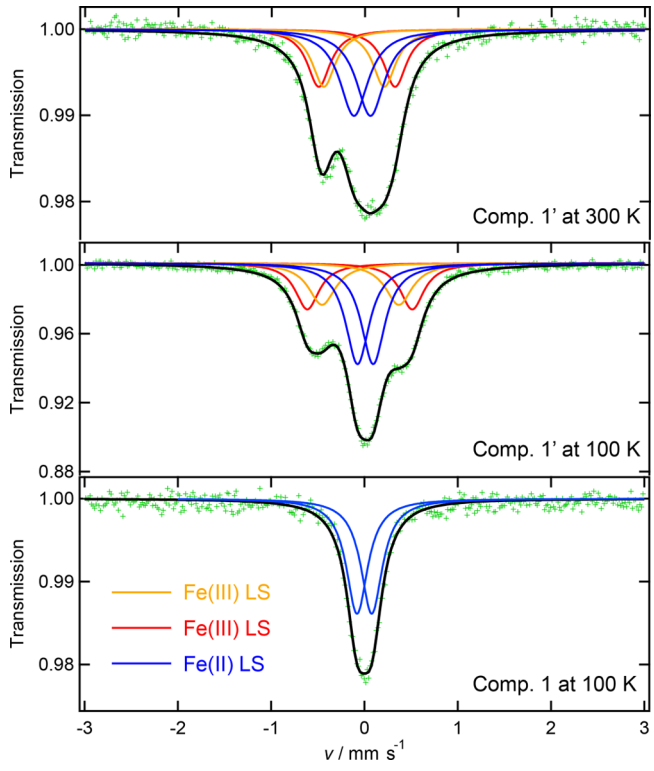


**Figure 3.** Mössbauer spectra of **1** at 100 K (bottom) and **1′** at 100 K (middle) and 300 K (top). The fitting parameters are given in Table S1 in the SI.


dx.doi.org/10.1021/ic500964m | Inorg. Chem. 2014, 53, 5899−5901

sample was revealed to be $(Et_4N)_2[\{Co(L^R)\}_6\{Fe(CN)_6\}_4](BF_4)\cdot 9H_2O$ (**1′**) by elemental analysis. The temperature-dependent magnetic susceptibility of **1′** is shown in Figure S1 in the Supporting Information (SI). The $\chi_m T$ values increased from 1.8 to 300 K, and no spin transition behavior was evident, with the $[Co^{II}(HS)_5Co^{III}(LS)Fe^{II}(LS)_2Fe^{III}(LS)_2]$ state stabilized across the full temperature range, a fact confirmed by Mössbauer spectra at 300 and 100 K (Figure 3; for parameters, see Table S1 in the SI). Structural analysis of the fresh sample at 100 K indicates the existence of many hydrogen-bonding interactions between terminal cyanide groups of the cage and solvent molecules (MeOH and $H_2O$). Hydrogen-bonded interactions affect the electronic states of the hexacyanoferrate units by exerting an electron-withdrawing effect that stabilizes the iron ions in their electron-rich divalent state.[14b,c] Desolvation destabilizes the low-temperature $[Co^{II}(HS)_3Co^{III}(LS)_3Fe^{II}(LS)_4]$ phase, resulting in the loss of ETCST activity.

In summary, an ETCST-active decanuclear cobalt−iron cluster was synthesized by the reaction of a chiral bidentate ligand with a cobalt source and hexacyanoferrate units. Temperature modulation induced magnetic and structural transitions resulting from electron transfer between neighboring metal ions. Such magnetically switchable chiral cage molecules will be investigated for their selective host−guest behavior and specific magnetooptical functionalities.

## ■ ASSOCIATED CONTENT

### Supporting Information

X-ray crystallographic data in CIF format and magnetic properties of dried sample **1′**. This material is available free of charge via the Internet at http://pubs.acs.org. CCDC 982659 and 982660 contain the supplementary crystallographic data for **1** at 100 and 291 K and can also be obtained free of charge from the Cambridge Crystallographic Data Centre via www.ccdc.cam.ac.uk/data_request/cif.

## ■ AUTHOR INFORMATION


### Corresponding Author

*E-mail: oshio@chem.tsukuba.ac.jp.


### Author Contributions

The manuscript was compiled from contributions by all authors.

### Notes

The authors declare no competing financial interest.

## ■ ACKNOWLEDGMENTS


We gratefully acknowledge a Grant-in-Aid for Scientific Research in Priority Area “Coordination Programming” (Area 2107) from MEXT, Japan, and a Grant-in-Aid for Scientific Research (Grant 25248014) from the JSPS.


## ■ REFERENCES


(1) Molecular-based functional materials: (a) Coskun, A.; Spruell, J. M.; Barin, G.; Dichtel, W. R.; Flood, A. H.; Botros, Y. Y.; Stoddart, J. F. *Chem. Soc. Rev.* **2012**, *41*, 4827−4859. (b) Yan, X.; Wang, F.; Zheng, B.; Huang, F. *Chem. Soc. Rev.* **2012**, *41*, 6042−6065.

(2) Lehn, J.-M. *Supramolecular Chemistry*; VCH: Weinheim, Germany, 1995.

(3) Cagelike compounds: (a) Fujita, M.; Tominaga, M.; Hori, A.; Therrien, B. *Acc. Chem. Res.* **2005**, *38*, 369−378. (b) Pluth, M. D.; Raymond, K. N. *Chem. Soc. Rev.* **2007**, *36*, 161−171. (c) Dalgarno, S. J.; Power, N. P.; Atwood, J. L. *Coord. Chem. Rev.* **2008**, *252*, 825−841. (d) Tranchemontagne, D. J.; Ni, Z.; O'Keeffe, M.; Yaghi, O. M. *Angew. Chem., Int. Ed.* **2008**, *47*, 5136−5147. (e) Chakrabarty, R.; Mukherjee, P. S.; Stang, P. J. *Chem. Rev.* **2011**, *111*, 6810−6918. (f) Ronson, T. K.; Zarra, S.; Black, S. P.; Nitschke, J. R. *Chem. Commun.* **2013**, *49*, 2476−2490.

(4) Grid compounds: (a) Ruben, M.; Rojo, J.; Romero-Salguero, F. J.; Uppadine, L. H.; Lehn, J.-M. *Angew. Chem., Int. Ed.* **2004**, *43*, 3644−3662. (b) Thompson, L. K.; Waldmann, O.; Xu, Z. *Coord. Chem. Rev.* **2005**, *249*, 2677−2690. (c) Dawe, L. N.; Shuvaev, K. V.; Thompson, L. K. *Chem. Soc. Rev.* **2009**, *38*, 2334−2359.

(5) Metal wires: (a) Bera, J. K.; Dunbar, K. R. *Angew. Chem., Int. Ed.* **2002**, *41*, 4453−4457. and references cited therein. (b) Kuo, J.-H.; Tsao, T.-B.; Lee, G.-H.; Lee, H.-W.; Yeh, C.-Y.; Peng, S.-M. *Eur. J. Inorg. Chem.* **2011**, *2011*, 2025−2029. (c) Barrios, L. A.; Aguilà, D.; Roubeau, O.; Gamez, P.; Ribas-Ariño, J.; Teat, S. J.; Aromí, G. *Chem.—Eur. J.* **2009**, *15*, 11235−11243.

(6) Rotaxanes: Nicholas, V.; Loeb, S. J. *Chem. Soc. Rev.* **2012**, *41*, 5896−5906 and references cited therein.

(7) Catenanes: Chambron, J.-C.; Sauvage, J.-P. *New J. Chem.* **2013**, *37*, 49−57 and references cited therein.

(8) Functional cage: (a) Yoshizawa, M.; Klosterman, J. K.; Fujita, M. *Angew. Chem., Int. Ed.* **2009**, *48*, 3418−3438 and references cited therein. (b) Han, M.; Michel, R.; He, B.; Chen, Y.-S.; Stalke, D.; John, M.; Clever, G. H. *Angew. Chem., Int. Ed.* **2013**, *52*, 1319−1322.

(9) Nanosized electronic devices: (a) Park, S.; Wang, G.; Cho, B.; Kim, Y.; Song, S.; Ji, Y.; Yoon, M.-H.; Lee, T. *Nat. Nanotechnol.* **2012**, *7*, 438−442. (b) Hong, S.; Grinolds, M. S.; Maletinsky, P.; Walsworth, R. L.; Lukin, M. D.; Yacoby, A. *Nano Lett.* **2012**, *12*, 3920−3924. (c) Loh, O. Y.; Espinosa, H. D. *Nat. Nanotechnol.* **2012**, *7*, 283−295.

(10) Metal wires in molecular electronics: (a) Chae, D.-H.; Berry, J. F.; Jung, S.; Cotton, F. A.; Murillo, C. A.; Yao, Z. *Nano Lett.* **2006**, *6*, 165−168. (b) Shih, K.-N.; Huang, M.-J.; Liu, H.-C.; Fu, M.-D.; Kuo, C.-K.; Huang, G.-C.; Lee, G.-H.; Chen, C.-h.; Peng, S.-M. *Chem. Commun.* **2010**, *46*, 1338−1340. (c) Chen, I.-W. P.; Fu, M.-D.; Tseng, W.-H.; Yu, J.-Y.; Wu, S.-H.; Ku, C.-J.; Chen, C.-h.; Peng, S.-M. *Angew. Chem., Int. Ed.* **2006**, *45*, 5814−5818.

(11) Champin, B.; Mobian, P.; Sauvage, J.-P. *Chem. Soc. Rev.* **2007**, *36*, 358−366.

(12) Harris, K.; Sun, Q.-F.; Sato, S.; Fujita, M. *J. Am. Chem. Soc.* **2013**, *135*, 12497−12499.

(13) Cyanide-bridged cage molecules: (a) Shiga, T.; Newton, G. N.; Mathieson, J. S.; Tetsuka, T.; Nihei, M.; Cronin, L.; Oshio, H. *Dalton Trans.* **2010**, *39*, 4730−4733. (b) Shiga, T.; Iijima, F.; Tetsuka, T.; Newton, G. N.; Oshio, H. *Macromol. Symp.* **2012**, *317−318*, 286−292.

(14) Co−Fe ETCST: (a) Nihei, M.; Sekine, Y.; Suganami, N.; Nakazawa, K.; Nakao, A.; Nakao, H.; Murakami, Y.; Oshio, H. *J. Am. Chem. Soc.* **2011**, *133*, 3592−3600. (b) Mitsumoto, K.; Oshiro, E.; Nishikawa, H.; Shiga, T.; Yamamura, Y.; Saito, K.; Oshio, H. *Chem.—Eur. J.* **2011**, *17*, 9612−9618. (c) Newton, G. N.; Mitsumoto, K.; Wei, R.-J.; Iijima, F.; Shiga, T.; Nishikawa, H.; Oshio, H. *Angew. Chem., Int. Ed.* **2014**, *53*, 2941−2944. (d) Hoshino, N.; Iijima, F.; Newton, G. N.; Yoshida, N.; Shiga, T.; Nojiri, H.; Nakao, A.; Kumai, R.; Murakami, Y.; Oshio, H. *Nat. Chem.* **2012**, *4*, 921−926. (e) Li, D.; Clérac, R.; Roubeau, O.; Harté, E.; Mathonière, C.; Bris, R. L.; Holmes, S. M. *J. Am. Soc. Chem.* **2008**, *130*, 252−258.


(15) Synthesis of **1**: To a mixture solution of 2-pyridinecarbaldehyde (71.1 μL, 0.75 mmol) and *R*-(+)-phenylethylamine (95.7 μL, 0.75 mmol) in methanol (3.0 mL) was added a solution of $Co(BF_4)_2\cdot 6H_2O$ (85.2 mg, 0.25 mmol) and $(Et_4N)_3[Fe(CN)_6]$ (301 mg, 0.50 mmol) in methanol (4.0 mL). The stirred mixture turned from dark red to dark green before it was filtered and left to crystallize by slow evaporation. Prismatic dark-green crystals, suitable for X-ray structural analysis, of **1** were collected by filtration and air-dried. Yield: 80.1 mg (43%). Elem anal. Calcd for $C_{208}H_{226}N_{50}BF_4O_9Co_6Fe_4$ (**1′**): C, 59.00; H, 5.38; N, 16.54. Found: C, 59.11; H, 5.38; N, 16.54. IR (KBr pellets, $cm^{-1}$): 2138, 2117, 2061, 2026, 1634, 1084.